MIT Libraries | DSpace@MIT

MIT Open Access Articles

Applicability and safety of dual-frequency ultrasonic treatment for the transdermal delivery of drugs

The MIT Faculty has made this article openly available. ***Please share*** how this access benefits you. Your story matters.

Citation: Schoellhammer, Carl M. et al. "Applicability and Safety of Dual-Frequency Ultrasonic Treatment for the Transdermal Delivery of Drugs." Journal of Controlled Release 202 (2015): 93–100.

As Published: http://dx.doi.org/10.1016/j.jconrel.2015.02.002

Publisher: Elsevier

Persistent URL: http://hdl.handle.net/1721.1/108647

Version: Author's final manuscript: final author's manuscript post peer review, without publisher's formatting or copy editing

Terms of use: Creative Commons Attribution-NonCommercial-NoDerivs License

Massachusetts Institute of Technology

Author Manuscript

Author Manuscript

Author Manuscript

Author Manuscript

HHS Public Access

Author manuscript

J Control Release. Author manuscript; available in PMC 2016 April 08.

Published in final edited form as:

J Control Release. 2015 March 28; 202: 93–100. doi:10.1016/j.jconrel.2015.02.002.

Applicability and safety of dual-frequency ultrasonic treatment for the transdermal delivery of drugs

Carl M. Schoellhammer[a,b], **Sharanya Srinivasan**[c], **Ross Barman**[b], **Stacy H. Mo**[a,b], **Baris E. Polat**[a], **Robert Langer**[a,b,*], and **Daniel Blankschtein**[a,**]

[a]Department of Chemical Engineering, Massachusetts Institute of Technology, Cambridge, MA 02139, USA

[b]The David H. Koch Institute for Integrative Cancer Research, Massachusetts Institute of Technology, Cambridge, MA 02139, USA

[c]Department of Biology, Massachusetts Institute of Technology, Cambridge, MA 02139, USA

Abstract

Low-frequency ultrasound presents an attractive method for transdermal drug delivery. The controlled, yet nonspecific nature of enhancement broadens the range of therapeutics that can be delivered, while minimizing necessary reformulation efforts for differing compounds. Long and inconsistent treatment times, however, have partially limited the attractiveness of this method. Building on recent advances made in this area, the simultaneous use of low- and high-frequency ultrasound is explored in a physiologically relevant experimental setup to enable the translation of this treatment to testing in vivo. Dual-frequency ultrasound, utilizing 20 kHz and 1 MHz wavelengths simultaneously, was found to significantly enhance the size of localized transport regions (LTRs) in both *in vitro* and *in vivo* models while decreasing the necessary treatment time compared to 20 kHz alone. Additionally, LTRs generated by treatment with 20 kHz + 1 MHz were found to be more permeable than those generated with 20 kHz alone. This was further corroborated with pore-size estimates utilizing hindered-transport theory, in which the pores in skin treated with 20 kHz + 1 MHz were calculated to be significantly larger than the pores in skin treated with 20 kHz alone. This demonstrates for the first time that LTRs generated with 20 kHz + 1 MHz are also more permeable than those generated with 20 kHz alone, which could broaden the range of therapeutics and doses administered transdermally. With regard to safety, treatment with 20 kHz + 1 MHz both *in vitro* and *in vivo* appeared to result in no greater skin disruption than that observed in skin treated with 20 kHz alone, an FDA-approved modality. This study demonstrates that dual-frequency ultrasound is more efficient and effective than single-frequency ultrasound and is well-tolerated *in vivo*.

Keywords

Cavitation; Dual-frequency; Skin; Sonophoresis; Transdermal drug delivery; Ultrasound

*Correspondence to: R. Langer, Department of Chemical Engineering, Room 76-661, Massachusetts Institute of Technology, 77 Massachusetts Avenue, Cambridge, MA 02139, USA. **Correspondence to: D. Blankschtein, Department of Chemical Engineering, Room 66-444, Massachusetts Institute of Technology, 77 Massachusetts Avenue, Cambridge, MA 02139, USA.

Supplementary data to this article can be found online at http://dx.doi.org/10.1016/j.jconrel.2015.02.002.

Author Manuscript Author Manuscript Author Manuscript Author Manuscript

1. Introduction

Non-invasive transdermal drug delivery (TDD) presents an attractive method for drug administration [1,2]. In addition to the potential benefits of patient compliance associated with painless drug delivery, TDD can reduce first-pass degradation of drugs typically associated with the oral route and enables the delivery of larger molecules limited to subcutaneous injection [1,2]. Despite countless experimental investigations surrounding this route, its use clinically is largely limited to the delivery of small molecules, such as nicotine and estradiol [3]. This is due in large part to the barrier posed by the outermost layer of the skin, the *stratum corneum* (SC). While there exist several methods to overcome or permeabilize this membrane, each method has associated limitations [4]. Treatment of skin with ultrasound (US) (also known as sonophoresis), for example, has the potential to permeabilize relatively large areas, but typically requires large, bulky equipment and a power source [5]. Recently, there has been renewed research interest in sonophoresis. Two major challenges limiting greater clinical use is the portability of the equipment required and the length of the treatment required [6,7]. Studies addressing the former hurdle have focused on the use of low-profile cymbal transducer arrays that can be integrated into patches [8,9]. In addition to portability, these devices minimize the excitation voltages required, reducing power consumption [10].

With regard to the treatment times necessary, a new approach has recently been investigated to increase permeabilization efficiency, thereby decreasing the required treatment time [11]. This method employs the use of two US frequencies simultaneously. A proof-of-concept study demonstrated that the use of both low- (<60 kHz) and high-frequency (>1 MHz) US together resulted in greater transient cavitation events, as assessed by pitting data, and resulted in larger localized transport regions (LTRs) *in vitro* [11].

While this initial study demonstrated that the simultaneous application of low- and high-frequency US could enhance cavitational activity, the experimental setup required submerging tissue in a tank to allow for both frequencies to be applied simultaneously. This setup could result in artificial enhancement in skin permeability due to the underside of the dermatomed skin layer (epidermis) being exposed to surfactant present in the coupling solution. Additionally, there has never been a mechanistic exploration of the permeability of the resulting LTRs or the safety and tolerability of this new method. Here, we build on this preliminary report of the use of dual-frequency US to first develop an experimental setup which exposes only the top surface of the skin to the coupling solution, while allowing for the simultaneous application of both 20 kHz and 1 MHz US. We then use this setup to explore LTR formation, investigate the mechanistic underpinnings of this modality, and quantify the resulting permeability of treated skin in vitro over a range of relevant treatment times. We also examine treated skin histologically to determine the level of barrier disruption as a result of the US treatment. Finally, we utilize this setup to allow for treatment *in vivo* in pigs to examine LTR formation and tolerability.

Author Manuscript Author Manuscript Author Manuscript Author Manuscript

2. Experimental section

2.1. Materials

All chemicals were used as received. Sodium lauryl sulfate (SLS), 4 kDa FITC-labeled dextran, and phosphate buffered saline (PBS) were obtained from Sigma-Aldrich Company (St. Louis, MO). Lysine-fixable 3, 10, and 70 kDa dextrans labeled with Texas Red were purchased from Invitrogen (Carlsbad, CA). Allura red was obtained from TCI America (Portland, OR).

2.2. Preparation of skin samples and ultrasonic treatment

All procedures were approved by the Massachusetts Institute of Technology Committee on Animal Care. Porcine skin was used because of its physiological similarity to human skin [12]. Skin was procured by Research 87 (Boylston, MA). The preparation and storage of skin samples followed previously published protocols [13]. Briefly, back and flank skin was dissected from female Yorkshire pigs within an hour of euthanization. This skin was sectioned into 25-mm wide strips and the subcutaneous fat was removed using a razor blade. The skin was then stored at−85 °C for up to six months. Prior to use in experiments, skin was thawed for 20 min in PBS and the hair was trimmed using surgical scissors. The skin was then dermatomed to 700 μm using an electric reciprocating dermatome (Zimmer Orthopedic Surgical Products, Dover, Ohio), and cut into 25 × 25-mm samples. The skin samples were then mounted in a custom diffusion cell to enable simultaneous sonication of the skin with both 20 kHz and 1 MHz US. Specifically, high vacuum grease (Dow Corning, Midland, MI) was applied to the flange of the custom-built top (FineLine Prototyping, Raleigh, NC) and 15-mm inner-diameter diffusion cell receiver chamber (PermeGear, Hellertown, PA). The skin was applied to the custom-designed top and then sandwiched between the top and receiver chamber. The top and bottom chambers were then clamped together and the receiver chamber was filled with PBS (12 mL) and a small volume of PBS was added to the custom-designed top to keep the skin hydrated until treatment.

Skin samples were treated in a similar fashion to previously reported methods [11,14,15]. Specifically, a 20 kHz horn (Sonics and Materials, Inc. Model VCX 500, Newtown, CT) and a 1 MHz horn (Therasound 3 Series, Richmar Corporation, Chattanooga, TN) were employed. The 20 kHz US horn was positioned 3 mm above the skin surface and operated at an intensity of 8 W/cm^2 (by calorimetry) and a 50% duty cycle (1 s on, 1 s off). The 1 MHz horn was placed on the side of the 20 kHz horn, approximately 5 cm from the leading edge of the skin. The 1 MHz horn was programmed to operate at a power of 2.0 W/cm^2 continuously. The custom diffusion top was filled with 300 mL of a solution of 1 wt.% SLS and 0.04 wt.% Allura red dye in PBS. The treatment times tested ranged between 4 and 8 min, which are within the range of commonly-tested treatment times in the literature [16,17]. Thermal effects were determined to be negligible as the temperature increase of the coupling solution was less than 2 °C even at the longest treatment time considered. Prior work has shown that an increase of at least 10 °C is necessary to appreciably permeabilize the skin [18]. Treatments utilizing 20 kHz US alone were used as a control throughout the study. The use of 1 MHz US alone was not tested because it has been established in the literature that high-frequency US (≥1 MHz) at typical intensities, such as those used here, do

Author Manuscript Author Manuscript Author Manuscript Author Manuscript

not generate transient cavitation [1]. As a result, there would not be any quantifiable LTR formation and the resulting flux of 4 kDa dextran would not be significantly different than that observed in native skin [18].

2.3. Skin resistivity measurements

Electrical resistivity has previously been shown to be an accurate measure of skin perturbation [15,19]. The resistivity across skin samples was determined using a method similar to previously published protocols [17,20]. Specifically, a 10 Hz sinusoidal wave with root-mean-square voltage of 100 mV was employed (Hewlett Packard Model 33120A, Palo Alto, CA). This signal was then applied across the skin using two Ag/AgCl electrodes (In Vivo Metric, Healdsburg, CA). The resulting current was measured using a multimeter (Fluke, Model 87 V, Everett, WA) and the resistance calculated using Ohm's Law. Finally, the resistivity was found by multiplying the resistance by the area of the skin exposed (the diffusion cells have an exposure area of 1.76 cm^2). In all measurements, the background resistance (resistance of PBS in the diffusion cell without skin) was accounted for by subtracting it from the resistance observed when the skin was mounted in the diffusion cell. All skin samples were ensured to have a starting resistivity of at least 35 k $\Omega \cdot cm^2$, otherwise, the skin sample was considered damaged and discarded [19].

2.4. Quantification of LTR area

Immediately after the US treatment, the coupling solution was discarded and the diffusion top and skin were washed thoroughly with PBS to remove any remaining coupling solution. The diffusion cell was then disassembled, the skin removed and placed on a paper towel, and blotted dry to prepare it for imaging. The skin was imaged using a digital camera (Panasonic DMC-ZS7, 12.1 megapixels, shutter speed 1/2000 s) positioned approximately 10 cm above the skin. The resulting image was then cropped making sure that only the portion of the skin exposed to US was captured (1.5 cm × 1.5 cm) and processed using ImageJ 1.46r (National Institutes of Health, Bethesda, MD). Specifically, the blue channel of the LTR image was isolated because it has been shown to give the best contrast between LTRs and non-LTRs [21]. The image was then inverted, and the average pixel intensity of non-LTRs was measured. This pixel intensity was subtracted from the entire image to account for variations in lighting at the time of imaging. The image was then re-inverted. The threshold was adjusted using the default value found by ImageJ. Finally, the LTR area was quantified using the “Analyze Particles” function.

2.5. Steady-state dextran permeability

Once the skin samples were imaged to quantify LTR size, they were remounted in clean diffusion cells using standard glass tops (PermeGear, Hellertown, PA), and filled with PBS. A magnetic stir bar was added to the receiver chamber. The donor chambers were filled with 1.5 mL of 0.1 wt.% 4 kDa dextran in PBS. The receiver chambers were magnetically stirred at 500 rpm. To ensure that the lag-phase was overcome, the receiver chambers were sampled between hours 20 and 48. For each sample, a 200 μL aliquot was taken and replaced with an equal volume of fresh PBS. These samples were then placed in 96-well plates and read using a plate reader (Tecan Infinite M200Pro) (excitation: 490 nm, emission: 525 nm). A known

Author Manuscript Author Manuscript Author Manuscript Author Manuscript

standard concentration series was also run to convert the sample emission to concentration. The permeability, P of dextran was then calculated using Eq. (1):

$$P=\frac{V_R}{AC_D}\frac{\Delta C_R}{\Delta t} \quad (1)$$

where V_R is the volume of the receiver chamber, A is the area for diffusion, C_D is the concentration of dextran in the donor chamber, and $\Delta C_R/\Delta t$ is the regression slope of a plot of the receiver chamber concentration with time.

2.6. Aqueous porous pathway model

Theoretical pore sizes were estimated using the aqueous porous pathway model [22]. This theory allows for the estimation of theoretical pores in a medium using the permeability of a molecule (calculated from Eq. (1)) and the electrical resistivity of the membrane upon the application of a current. Assuming that both the permeant and the ions traverse the same pathway through the skin, a hindrance factor may be calculated for the permeant from known relations [23].

The permeability (P) and electrical resistivity (R) are related by Eq. (2):

$$\log(P)=\log(C)-\log(R) \quad (2)$$

where C is a constant given by:

$$C=\frac{kT}{2z^2Fc_{\text{ion}}e}\frac{D^{\infty}_{\text{permeant}}H\left(\lambda_{\text{permeant}}\right)}{D^{\infty}_{\text{ion}}H(\lambda_{\text{ion}})}. \quad (3)$$

In Eq. (3), k is the Boltzmann's constant, T is the absolute temperature, z is the valence of the electrolyte, F is the Faraday's constant, c_{ion} is the molar concentration of the electrolyte, e is the electronic charge, D^{∞} is the diffusion coefficient of either the permeant or the ion at infinite dilution, λ is the ratio of the radius of either the permeant or the ion to the radius of the aqueous pores in the skin, and $H(\lambda)$ is the hindrance factor for the permeant or the ion [22].

The relation for the hindrance factor is given by [24]:

$$H(\lambda)=1+\frac{9}{8}\lambda\ln(\lambda)-1.56034\lambda+0.528155\lambda^2+1.91521\lambda^3-2.81903\lambda^4+0.270788\lambda^5+1.10115\lambda^6-0.435933\lambda^7. \quad (4)$$

Once C is determined from Eq. (2), the only unknown quantity present is the skin pore radius in the ratio of the hindrance factors in Eq. (3). It is important to note that there is an upper limit on the pore size that can be estimated using Eq. (4) based on the permeant selected. The permeant must experience some amount of hindrance as a result of traversing the pores. Because the hindrance factor ranges from 0 to 1 (1 representing no hindrance), an upper limit is set on $H(\lambda)$, above which the pores are considered to be too large to estimate. Here, in this report, the upper limit on the hindrance factor is $H(\lambda) = 0.9$, which has been

Author Manuscript Author Manuscript Author Manuscript Author Manuscript

used previously in the literature [22,23]. The hydrodynamic radius of 4 kDa dextran is 14 Å. This yields an upper limit on pore size estimates of approximately 870 Å [25]. Finally, the applicability of this theory to pore size estimates in skin has previously been tested by plotting log(P) versus log(R) and requiring that the 95% confidence interval of the regression slope contains the theoretical value of −1 (see Eq. (2)). Previous work has shown this requirement to hold, and here too, it was ensured that the 95% confidence interval of the regression slope contained the value of −1 [15].

2.7. Histology

Individual skin samples were either treated with 20 kHz alone or with 20 kHz + 1 MHz as described in Section 2.2. After treatment, these samples were removed from the diffusion cell, washed, and blotted dry. The area exposed to the coupling solution and the US was isolated using a scalpel. The treated area was then sliced into 2 mm-wide sections and fixed overnight in 10% formalin. The skin sections were then mounted in paraffin blocks to allow cross sections of the skin to be taken. Two, 8 μm-thick sections separated by a 200 μm step were stained with hematoxylin and eosin and mounted to glass microscope slides for histological examination.

2.8. Dextran diffusion depth

While the US treatment increases the permeability of the skin, there may still exist limitations on the molecular weight of molecules that can diffuse through treated skin. To better understand this size-dependent permeability, dextrans of various sizes labeled with Texas red were allowed to diffuse through treated skin for a set period of time. Specifically, 3, 10, and 70 kDa dextrans labeled with Texas Red were used to image the relative penetration depth of these molecules into the skin. Skin was treated as described in Section 2.2 for 6 or 8 min. Additionally, untreated skin samples were included as a control. After treatment, the skin samples were mounted in fresh diffusion cells with a magnetic stir bar in the receiver chamber. Only one molecule was allowed to diffuse through any given skin sample. 1-mL of 3, 10, or 70 kDa dextran solution at a concentration of 1 mg/mL in PBS was added to the donor chamber and the receiver chamber was stirred at 500 rpm. The dye was allowed to diffuse for only 1 h to ensure that the diffusion front would not reach the receiver chamber. At that point, the dye solution was removed and the skin thoroughly washed with PBS. The skin was then sectioned and fixed overnight in 10% formalin. Mounting and processing was performed as described in Section 2.7 with the exception that the skin was unstained.

The slides were imaged by the microscopy core facility in the Swanson Biotechnology Center (Massachusetts Institute of Technology). Briefly, slides were imaged with an Olympus FV-1000MP multiphoton microscope with a 25×, 1.05 N.A. objective. Samples were excited at 860 nm using a Ti-Sapphire pulsed laser (Spectra-Physics, Santa Clara, CA). Emission for Texas red was collected with a 607/70 nm band-pass filter and collagen was imaged by second harmonic generation at 430 nm. Individual image channels were combined in ImageJ.

Author Manuscript Author Manuscript Author Manuscript Author Manuscript

2.9. In vivo experiments

All procedures were conducted in accordance with the protocols approved by the Massachusetts Institute of Technology Committee on Animal Care. Female Yorkshire pigs approximately 50 kg in size were used for *in vivo* testing. Anesthesia was induced with intramuscular injection of 5 mg/kg Telazol and 2 mg/kg xylazine. A 20 gauge peripheral venous catheter was then placed in a vein in the ear of the animals. Anesthesia was maintained with 1 mg/kg ketamine and 0.3 mg/kg midazolam intravenously. The animals were laid on their side. The hair on the flank of the animal was carefully trimmed away using surgical scissors so as to not damage the skin. The custom-built top was then affixed to the skin using high vacuum grease. Treatment was performed following methods described in Section 2.2 with the addition of a plastic spacer connecting the diffusion top to the 20 kHz horn to maintain a distance of 3 mm from the horn tip to the skin. In this manner, position variability due to breathing of the animal is minimized. Six and eight minute treatments were tested.

Following treatment, the diffusion top was removed and the skin washed with water to remove any excess coupling solution and gently blotted dry. The resulting LTRs were imaged and quantified according to the procedure described in Section 2.4. Once the LTRs were imaged, a biopsy was taken for the purpose of histological examination using a punch biopsy with a 3 mm diameter (Miltex, York, PA). The biopsies were fixed in 10% formalin. Histological slides were prepared as described in Section 2.7.

2.10. Statistical significance

Statistical significance was defined throughout as $P < 0.05$. *P*-values were determined by one-way analysis-of-variance with multiple comparison testing unless otherwise noted. All calculations were performed in MatLab R2014a (MathWorks, Natick, MA).

3. Results and discussion

3.1. In vitro results

To better understand enhancement in skin permeability as a result of the simultaneous use of 20 kHz + 1 MHz US, a more relevant experimental setup had to be designed to allow for the simultaneous application of both low- and high-frequency US. A custom-built top was designed in AutoCAD 2012 (see Fig. 1A).

The top was designed so as to allow for unhindered bubble nucleation over the skin by the 1 MHz US horn. It was found that the top allowed for bubbles nucleated by the 1 MHz horn to oscillate over the area of the skin (Fig. 1B).

Once the top was determined not to hinder bubble formation by the 1 MHz horn, porcine skin samples were treated *in vitro* with the diffusion top and the resulting LTR areas quantified. LTR sizes as a result of either 20 kHz or 20 kHz + 1 MHz US are shown in Fig. 2A.

As shown in Fig. 2A, a 2.5-fold and nearly 6-fold enhancement in LTR size was observed at treatment times of 6 and 8 min, respectively, using both US frequencies simultaneously ($P <$

Author Manuscript Author Manuscript Author Manuscript Author Manuscript

0.0043). No significant difference in LTR size was observed at the shortest treatment time. Additionally, no significant difference was found between LTR sizes at any treatment time using 20 kHz US alone. This is in clear contrast to what was found using 20 kHz + 1 MHz, in which there is a statistically significant increase in LTR size with increasing treatment time ($P < 0.048$). In this new study, longer treatment times were required compared to the previously published report. This is a result of the experimental setup that was employed in the preliminary report [11]. Specifically, that study employed a tank to allow for skin samples to be exposed to 20 kHz and 1 MHz simultaneously. While treatment utilizing 20 kHz alone was included as a control in that study to validate the phenomenon of enhanced cavitational activity using dual-frequency US, submersion of skin samples in the tank exposed the underlying epidermis to the coupling fluid containing SLS [11]. This results in additional permeabilization of the skin. Therefore, in this present study, the treatment times examined were increased by 2 min. The setup reported here is a more physiologically relevant setup and now allows for testing of dual-frequency US *in vivo*, which was not previously possible. Aside from the increased treatment time required in this study, the general trend of LTR enhancement as a result of treatment with 20 kHz + 1 MHz compared to 20 kHz alone is in good agreement with that presented previously [11].

Next, the flux of 4 kDa dextran and theoretical pore sizes of treated skin were determined for treatment times of 6 and 8 min. Fluxes are shown in Fig. 2B and pore sizes in Table 1.

A statistically significant increase in the flux of 4 kDa dextran was observed by using 20 kHz + 1 MHz as opposed to 20 kHz alone ($P = 0.0012$ and 1.25×10^{-6} for 6 and 8 min treatments, respectively). Again, there was a statistical difference between the flux observed for samples treated with 20 kHz + 1 MHz for 6 or 8 min ($P = 0.009$), but no increase in flux with treatment time for the use of 20 kHz alone. Interestingly, the enhancement in flux at both treatment times using 20 kHz + 1 MHz was greater than that which would be expected based on the increase in LTR sizes alone at each treatment time. The dextran flux was 3.5- and 7.1-fold greater using 20 kHz + 1 MHz at 6 and 8 min, respectively, compared to the use of 20 kHz alone, while LTR area increased 2.5- and 6-folds respectively. Specifically, regression slope analysis of plots of permeability (from Eq. (1)) vs. LTR area demonstrated a greater increase in permeability per increase in LTR area through the use of 20 kHz + 1 MHz at both six and eight minute treatment times. Moreover, at each treatment time, the 95% confidence interval of the regression slopes does not overlap. This would suggest that LTRs generated by 20 kHz + 1 MHz are more permeable than those generated with 20 kHz alone.

This result is further supported by the pore size estimates utilizing the aqueous porous pathway model (Table 1). While the average theoretical pore size generated in samples treated with 20 kHz US was less than 81 Å, even the lower estimate of the pore sizes generated in samples treated with 20 kHz + 1 MHz was larger than the limit of detection (870 Å). These theoretical pore sizes can be attributed to the LTRs because the pore sizes of non-LTRs have previously been shown to be nearly identical to those found in untreated skin [23]. Because this previous result was found using a smaller permeant (calcein), a larger distribution of skin pores could be sampled by the permeant (on account of its smaller size), which would result in larger pore size estimates. As a result, it is reasonable to assume that

Author Manuscript Author Manuscript Author Manuscript Author Manuscript

the majority of the 4 kDa dextran would diffuse through the LTRs and therefore, the pore sizes calculated would more greatly reflect pore sizes within the LTRs. Further, there was no statistical difference between the pore sizes found as a result of six or eight minute treatments with 20 kHz alone (two-tailed Student's *T*-test).

The finding that the enhancement in permeability is greater than that observed in LTR size is a new and surprising result not previously explored using steady-state permeation studies. Indeed, the opposite result was previously reported, demonstrating a greater enhancement in LTR formation than in the delivery of model permeants [11]. This previous finding was hypothesized to be a result of larger molecules only having the capacity to "sample" pores large enough to diffuse through, with 20 kHz + 1 MHz treatment having no effect on the size of pores generated in the skin. This finding could potentially have been due to the artificial enhancement in permeability stemming from the experimental setup employed masking the true enhancement in permeability gained through the use of 20 kHz + 1 MHz US. Regardless of the reason, the data reported here unequivocally demonstrate that treatment with 20 kHz + 1 MHz does in fact increase pore size, resulting in a greater enhancement in permeability than in LTR size.

Further exploring the increase in pore size as a result of treatment with 20 kHz + 1 MHz US, the diffusion of 3, 10, and 70 kDa dextran labeled with Texas red was visualized by microscopy (Supplementary Fig. 1). Qualitatively, examination of skin samples treated with 20 kHz + 1 MHz showed greater penetration of 3, 10, and even 70 kDa dextran compared to skin treated with 20 kHz alone. As expected, there was negligible penetration of any molecule into untreated skin. Discernable diffusion of macromolecules into skin in a relatively short diffusion time is exciting and could potentially allow for a broader range of therapeutics to be administered transdermally.

In addition to the permeability enhancement capabilities of the simultaneous use of 20 kHz + 1 MHz US, the safety of this method was also assessed through histological examination of treated skin. All histology samples were examined by a pathologist in a blinded fashion to assess the location, extent, and severity of any disruption to normal tissue architecture. Representative skin histology images are shown in Fig. 3.

As expected, histological damage was noted to scale with treatment time regardless of the frequencies employed. Ablation of the SC was noted in all samples in discrete, sporadic areas. At treatment times of 6 and 8 min, there were ablative effects noted in the viable epidermis, and superficial dermis in a localized manner. This was determined by the observation of minor coagulation of collagen in the superficial layer of the dermis making distinction of individual fibers impossible. This was observed in both samples treated with 20 kHz and 20 kHz + 1 MHz US. Further, samples treated for 6 and 8 min showed evidence of vacuole formation in the epidermis and dermis and minor coagulative necrosis was observed sporadically throughout the dermis. These observations have previously been noted in the literature [26]. Importantly, there was no quantifiable difference in the extent or severity of tissue disruption between samples treated with 20 kHz and those treated with 20 kHz + 1 MHz at each treatment time considered. The fact that 20 kHz + 1 MHz US results

Author Manuscript Author Manuscript Author Manuscript Author Manuscript

in similar skin disruption as that resulting from treatment with 20 kHz alone, is reassuring, considering that the latter is an FDA-approved modality for the delivery of lidocaine [27].

3.2. In vivo results

Based on the significant enhancement observed at treatment times of 6 and 8 min *in vitro* and the likely safety of this method, this new treatment regimen was translated to *in vivo* testing in Yorkshire pigs. LTR formation and histological examination were performed to ascertain if the enhancement observed *in vitro* would persist in an *in vivo* system. The sizes of LTRs as a result of treatment are shown in Fig. 4.

The trends in LTR formation observed *in vivo* are in good agreement with those found *in vitro*. Treatment with 20 kHz + 1 MHz US resulted in statistically larger LTRs compared to those generated with the use of 20 kHz alone at both treatment times tested ($P \leq 0.032$). Moreover, similar to the *in vitro* results, the size of LTRs generated with 20 kHz US alone at 6 and 8 min was not statistically different ($P = 0.73$). Additionally, LTR formation using 20 kHz + 1 MHz US for 6 min was again larger, on average, than that resulting from 8 min of treatment using 20 kHz alone. This further confirms the fact that 20 kHz + 1 MHz US enables the reduction of treatment times to achieve comparable LTR sizes. Reducing the required treatment time will make US-assisted transdermal drug delivery more convenient, potentially enabling broader clinical use.

Clinical monitoring of the pigs over the period of a week post treatment showed the animals to be free of distress. Further, the area of the skin that was treated appeared healthy and uninfected. The treated area was undistinguishable from the surrounding tissue within four days posttreatment and identification of the treated area at earlier times posttreatment was only possible because of the presence of the Allura red dye staining the LTRs (see Fig. 5). Histological examination of the skin demonstrated sporadic ablation of the SC, epidermis and dermis in addition to minor vacuole formation and coagulative necrosis sporadically thought the upper layers of the dermis (see Fig. 6). The extent of skin injury was comparable to that observed in tissue treated *in vitro*. Finally, the extent and severity of tissue injury again could not be differentiated between those samples treated with 20 kHz or 20 kHz + 1 MHz US. Based on histological examination, treatments should likely be less than 8 min so that the treatment minimizes disruption to the dermis.

One interesting feature noted during histological examination of the tissue was the pattern of tissue ablation observed in skin samples treated with 20 kHz + 1 MHz US. As it can be seen in Fig. 6, portions of viable epidermis appear to have been ablated without ablation of the SC in samples treated with 20 kHz + 1 MHz US. This might suggest that transient cavitation is occurring within the skin. Cavitation within the skin has previously been hypothesized to play a significant role in low-frequency US and high-frequency US has been shown to produce stable cavitation within the skin [18,28]. Perhaps, under the influence of the 20 kHz horn, cavitation bubbles within the skin are now growing to unstable sizes, resulting in transient cavitation within the skin. This would be an interesting new area of study and would present a new phenomenon in US-mediated transdermal drug delivery.

Author Manuscript Author Manuscript Author Manuscript Author Manuscript

4. Conclusions

This study investigated the simultaneous use of 20 kHz + 1 MHz US for the purpose of transdermal drug delivery *in vitro* and *in vivo* in Yorkshire pigs. LTR formation as a result of 20 kHz + 1 MHz was found to be enhanced compared to 20 kHz alone at treatment times of 6 and 8 min. It was further found that utilizing 20 kHz + 1 MHz could decrease the required treatment time to achieve a certain LTR size. Additionally, LTRs formed as a result of treatment with 20 kHz + 1 MHz US were found to be more permeable than those formed with 20 kHz US alone. This was hypothesized to be due to enhanced cavitational activity, resulting in the estimation of larger pore sizes present in skin treated with 20 kHz + 1 MHz utilizing hindered-transport theory. Despite this greater permeability, histological examination of skin treated with 20 kHz + 1 MHz US *in vitro* and *in vivo* showed no greater disruption of viable tissues compared to the use of 20 kHz US alone, an FDA approved modality. Animals treated with 20 kHz + 1 MHz showed no clinical signs of distress and the treated area remained free of infection. The significant improvement in performance utilizing dual-frequency US should motivate further investigation into this method.

Supplementary Material

Refer to Web version on PubMed Central for supplementary material.

Acknowledgments

This work was funded in part by NIH grant EB-00351 (to R.L.) and NIH grant CA014051 for the Hope Babette Tang (1983) Histology Facility. The authors would like to thank Kathleen S. Cormier and Michael Brown for their help in preparing histology slides and Dr. Roderick T. Bronson for evaluating the histology. The authors also wish to thank Jeffrey Wyckoff of the microscopy core facility in the Swanson Biotechnology Center for imaging skin samples, and Morgan Jamiel for assistance with the in vivo experiments.

References

1. Prausnitz MR, Langer R. Transdermal drug delivery. Nat. Biotechnol. 2008 Nov.26(11):1261–1268. [PubMed: 18997767]
2. Schoellhammer CM, Blankschtein D, Langer R. Skin permeabilization for transdermal drug delivery: recent advances and future prospects. Expert Opin. Drug Deliv. 2014 Jan.11(3):393–407. [PubMed: 24392787]
3. Watkinson AC. A commentary on transdermal drug delivery systems in clinical trials. J. Pharm. Sci. 2013 Sep.102(9):3082–3088. [PubMed: 23468246]
4. Prausnitz MR, Mitragotri S, Langer R. Current status and future potential of transdermal drug delivery. Nat. Rev. Drug Discov. 2004 Feb.3(2):115–124. [PubMed: 15040576]
5. Polat BE, Hart D, Langer R, Blankschtein D. Ultrasound-mediated transdermal drug delivery: mechanisms, scope, and emerging trends. J. Control. Release. 2011 Jun.152(3):330–348. [PubMed: 21238514]
6. Smith NB. Perspectives on transdermal ultrasound mediated drug delivery. Int. J. Nanomedicine. 2009 Apr.2(4):585–594. [PubMed: 18203426]
7. Ogura M, Paliwal S, Mitragotri S. Low-frequency sonophoresis: current status and future prospects. Adv. Drug Deliv. Rev. 2008 Jun.60(10):1218–1223. [PubMed: 18450318]
8. Sunny Y, Bawiec CR, Nguyen AT, Samuels JA. Optimization of un-tethered, low voltage, 20–100 kHz flexural transducers for biomedical ultrasonics applications. Ultrasonics. 2012; 52(7):943–948. [PubMed: 22513259]

Author Manuscript Author Manuscript Author Manuscript Author Manuscript

9. Park E-J, Werner J, Beebe J, Chan S, Smith NB. Noninvasive ultrasonic glucose sensing with large pigs (~200 pounds) using a lightweight cymbal transducer array and biosensors. J. Diabetes Sci. Technol. 2009 Apr.3(3):517–523. [PubMed: 20144290]
10. Bawiec CR, Sunny Y, Nguyen AT, Samuels JA. Finite element static displacement optimization of 20–100 kHz flexural transducers for fully portable ultrasound applicator. Ultrasonics. 2013; 53(2): 511–517. [PubMed: 23040829]
11. Schoellhammer CM, Polat BE, Mendenhall J, Maa R, Jones B, Hart DP, Langer R, Blankschtein D. Rapid skin permeabilization by the simultaneous application of dual-frequency, high-intensity ultrasound. J. Control. Release. 2012; 163(2):154–160. [PubMed: 22940128]
12. Debeer S, Le Luduec J-B, Kaiserlian D, Laurent P, Nicolas J-F, Dubois B, Kanitakis J. Comparative histology and immunohistochemistry of porcine versus human skin. Eur. J. Dermatol. 2013; 23(4):456–466. [PubMed: 24047577]
13. Seto JE, Polat BE, Lopez RFV, Blankschtein D, Langer R. Effects of ultrasound and sodium lauryl sulfate on the transdermal delivery of hydrophilic permeants: comparative in vitro studies with full-thickness and split-thickness pig and human skin. J. Control. Release. 2010 Jul.145(1):26–32. [PubMed: 20346994]
14. Terahara T, Mitragotri S, Kost J, Langer R. Dependence of low-frequency sonophoresis on ultrasound parameters; distance of the horn and intensity. Int. J. Pharm. 2002; 235:35–42. [PubMed: 11879737]
15. Polat BE, Seto JE, Blankschtein D, Langer R. Application of the aqueous porous pathway model to quantify the effect of sodium lauryl sulfate on ultrasound-induced skin structural perturbation. J. Pharm. Sci. 2010 Oct.100(4):1387–1397. [PubMed: 20963845]
16. Polat BE, Deen WM, Langer R, Blankschtein D. A physical mechanism to explain the delivery of chemical penetration enhancers into skin during transdermal sonophoresis — insight into the observed synergism. J. Control. Release. 2012 Mar.158(2):250–260. [PubMed: 22100440]
17. Kushner J, Blankschtein D, Langer R. Evaluation of hydrophilic permeant transport parameters in the localized and non-localized transport regions of skin treated simultaneously with low-frequency ultrasound and sodium lauryl sulfate. J. Pharm. Sci. 2007; 97(2):906–918. [PubMed: 17887123]
18. Mitragotri S, Edwards DA, Blankschtein D, Langer R. A mechanistic study of ultrasonically-enhanced transdermal drug delivery. J. Pharm. Sci. 1995 Jun.84(6):697–706. [PubMed: 7562407]
19. Kasting GB, Bowman LA. DC electrical-properties of frozen, excised human skin. Pharm. Res. 1990 Feb.7(2):134–143. [PubMed: 2308893]
20. Mitragotri S, Farrell J, Tang H, Terahara T, Kost J, Langer R. Determination of threshold energy dose for ultrasound-induced transdermal drug transport. J. Control. Release. 2000; 63(1):41–52. [PubMed: 10640579]
21. Kushner J, Blankschtein D, Langer R. Experimental demonstration of the existence of highly permeable localized transport regions in low-frequency sonophoresis. J. Pharm. Sci. 2004; 93(11): 2733–2745. [PubMed: 15389675]
22. Tang H, Mitragotri S, Blankschtein D. Theoretical description of transdermal transport of hydrophilic permeants: application to low-frequency sonophoresis 2001 Journal of Pharmaceutical Sciences. J. Pharm. Sci. 2001; 90(5):545–568. [PubMed: 11288100]
23. Polat BE, Figueroa PL, Blankschtein D, Langer R. Transport pathways and enhancement mechanisms within localized and non-localized transport regions in skin treated with low-frequency sonophoresis and sodium lauryl sulfate. J. Pharm. Sci. 2010 Aug.100(2):512–529. [PubMed: 20740667]
24. Dechadilok P, Deen WM. Hindrance factors for diffusion and convection in pores. Ind. Eng. Chem. Res. 2006; 45(21):6953–6959.
25. Yuan W, Lv Y, Zeng M, Fu BM. Non-invasive measurement of solute permeability in cerebral microvessels of the rat. Microvasc. Res. 2009 Mar.77(2):166–173. [PubMed: 18838082]
26. Miller D, Smith N, Bailey M, Czarnota G, Hynynen K, Makin I. American Institute of Ultrasound in Medicine Bioeffects Committee, Overview of Therapeutic Ultrasound Applications and Safety Considerations. J. Ultrasound Med. 2012 Apr.31(4):623–634. [PubMed: 22441920]

Author Manuscript Author Manuscript Author Manuscript Author Manuscript

27. Polat BE, Blankschtein D, Langer R. Low-frequency sonophoresis: application to the transdermal delivery of macromolecules and hydrophilic drugs. Expert Opin. Drug Deliv. 2010 Dec.7(12): 1415–1432. [PubMed: 21118031]

28. Lavon I, Grossman N, Kost J, Kimmel E, Enden G. Bubble growth within the skin by rectified diffusion might play a significant role in sonophoresis. J. Control. Release. 2007 Feb.117(2):246–255. [PubMed: 17197050]

Author Manuscript Author Manuscript Author Manuscript Author Manuscript

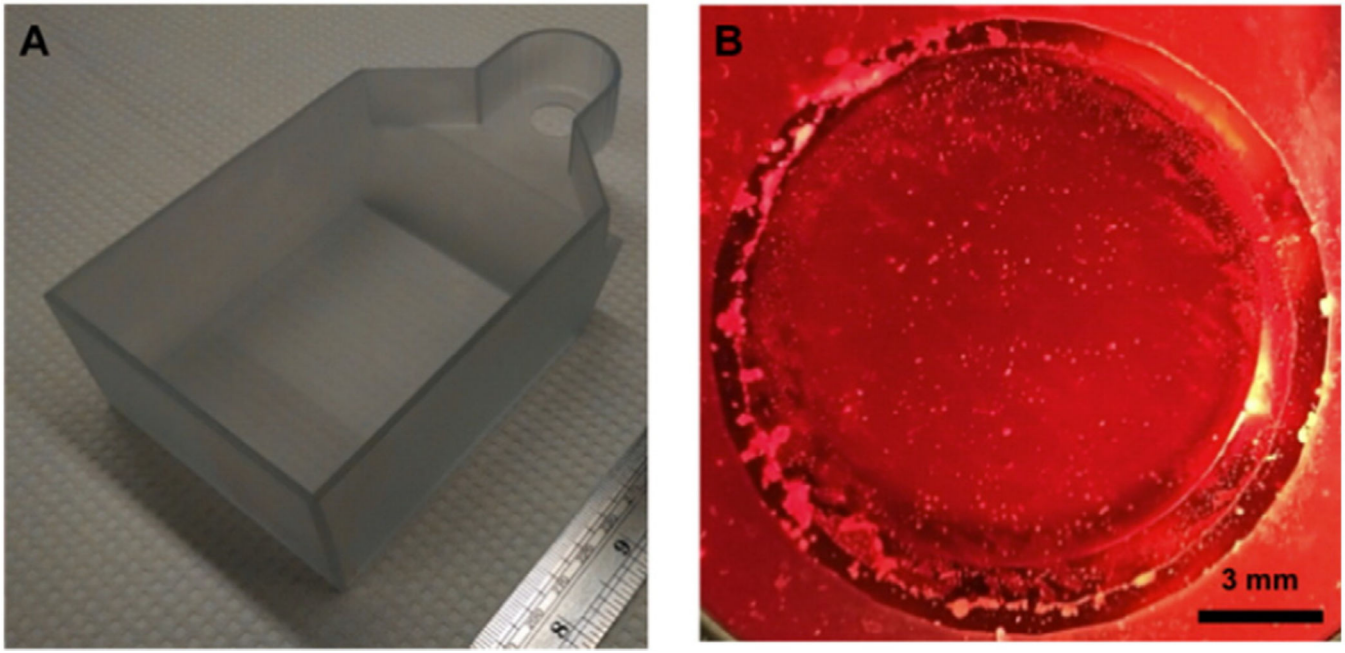

Fig. 1.

A) Custom designed diffusion top used for the study to allow for the simultaneous application of the 20 kHz and 1 MHz US horns. B) View from below the diffusion top looking up through the opening where the skin is normally mounted showing significant bubble formation when the 1 MHz US horn is on. The diffusion top is filled with a coupling solution of 1 wt.% SLS and 0.04 wt.% Allura red in PBS.

Author Manuscript
Author Manuscript
Author Manuscript
Author Manuscript

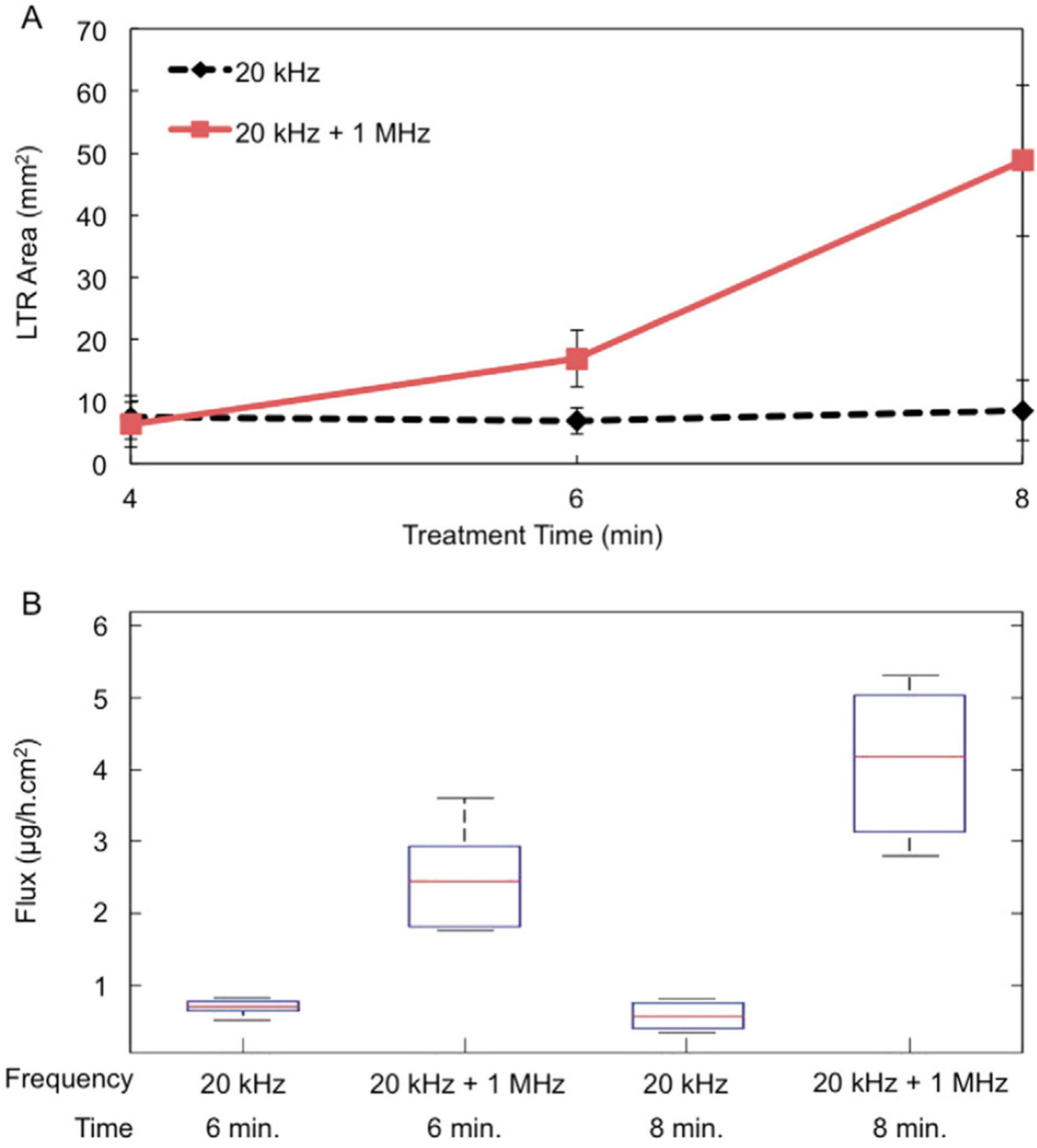

Fig. 2.

A) *In vitro* LTR size vs. treatment time as a result of treatment with either 20 kHz or 20 kHz + 1 MHz US. Each point represents n ≥ 3 biological repeats. Averages and standard deviations are presented. B) Flux of 4 kDa dextran at steady-state as a result of the US treatment for either 6 or 8 min. The median, 25th, and 75th percentiles are shown. Whiskers indicate the most extreme data points. Each condition represents n ≥ 5 biological repeats.

Author Manuscript Author Manuscript Author Manuscript Author Manuscript

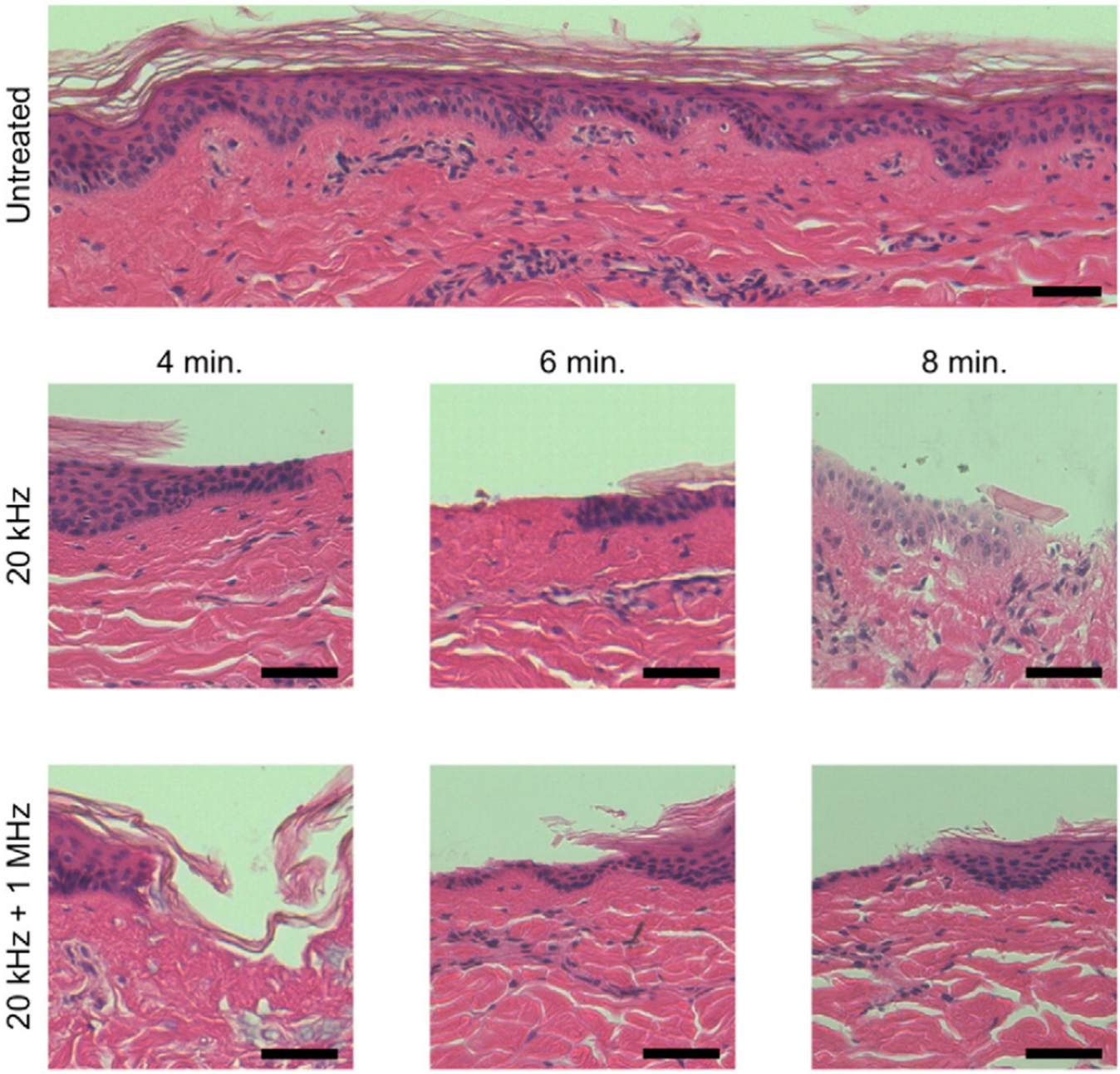

Fig. 3.

Representative images of the histological view of *in vitro*-treated porcine skin. Skin that was dermatomed and then immediately fixed in formalin is shown as the control. The scale bar in all images is 50 μm.

Author Manuscript Author Manuscript Author Manuscript Author Manuscript

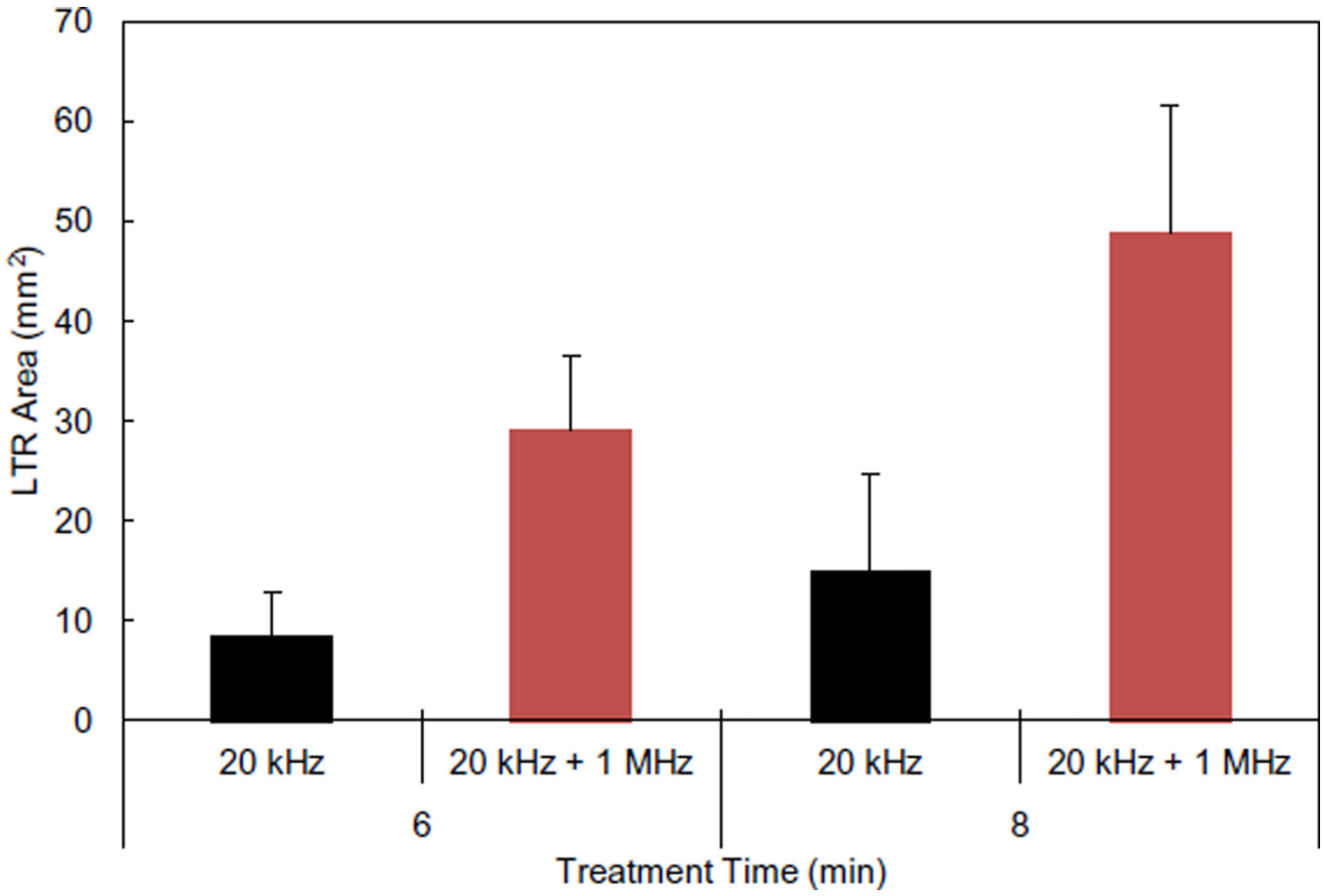

Fig. 4.

In vivo LTR sizes as a result of treatment with either 20 kHz US or 20 kHz + 1 MHz US. Each condition represents n = 4 biological repeats. Averages and standard deviations are presented.

Author Manuscript Author Manuscript Author Manuscript Author Manuscript

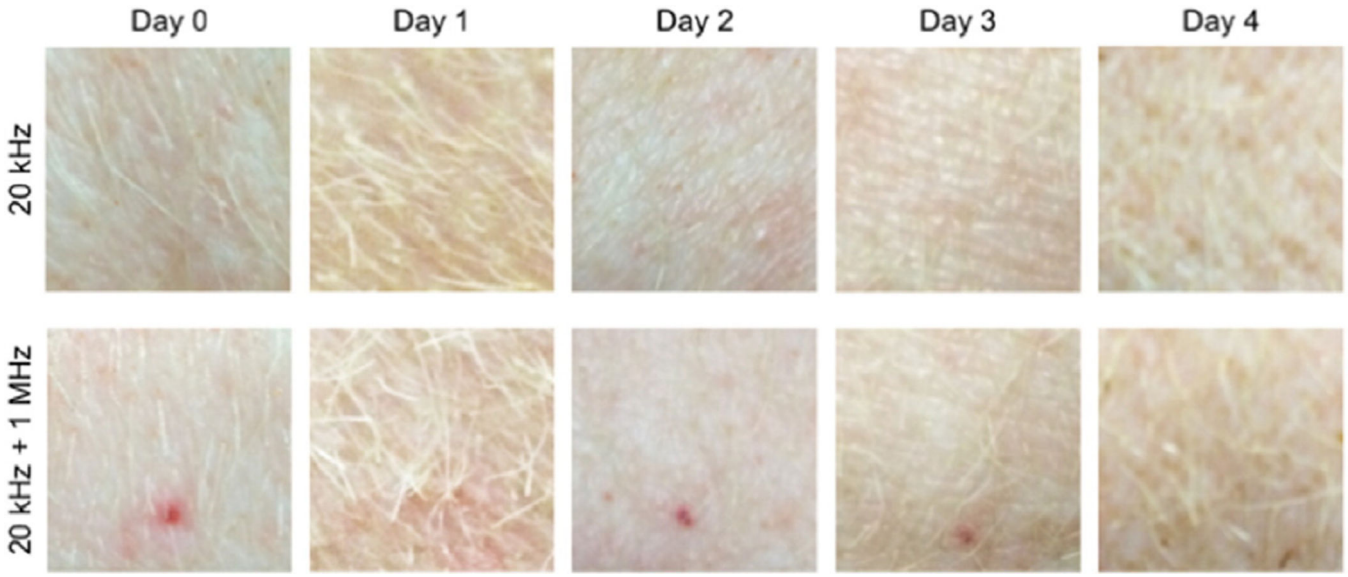

Fig. 5.

Images of the sites of the US treatment *in vivo* over time. Images on Day 0 were taken immediately after the US treatment. Image brightness has been adjusted to account for differences in lighting on subsequent days. Each image is 15 × 15 mm.

Author Manuscript Author Manuscript Author Manuscript Author Manuscript

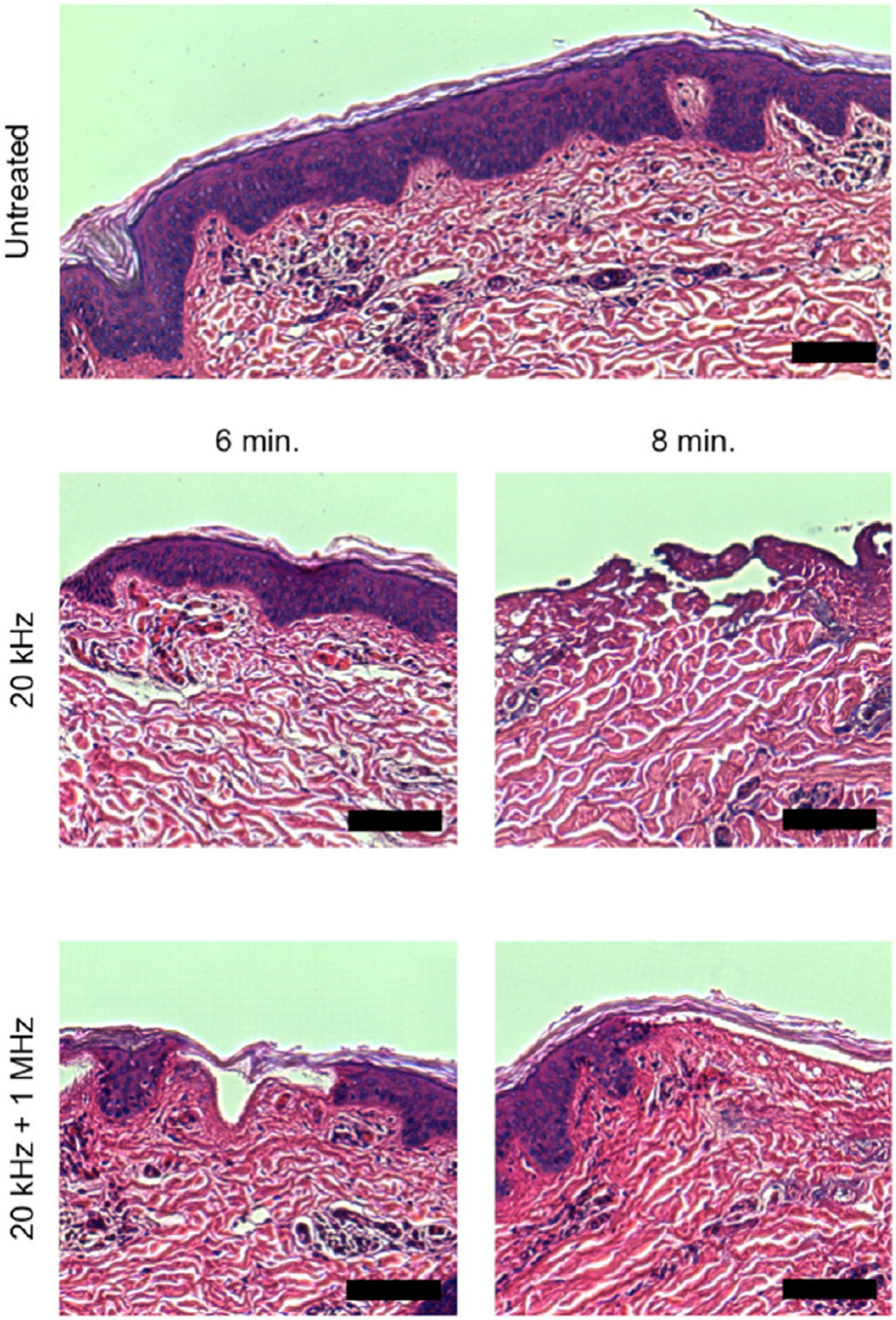

Fig. 6.

Representative images of the histological view of *in vivo*-treated porcine skin. The scale bar in all images is 100 μm.

Author Manuscript Author Manuscript Author Manuscript Author Manuscript

Table 1

Pore radius estimates using the aqueous porous pathway model. The average, lower, and upper limits on pore size are based on the average and 95% confidence interval for C in Eq. (3).

Treatment time (min)	r_{pore} (Å)					
	20 kHz			20 kHz + 1 MHz		
	Lower	Average	Upper	Lower	Average	Upper
6	69.07	80.57	95.2	>870	>870	>870
8	55.57	64.67	75.9	>870	>870	>870